New forms of deuteron equations and wave function representations

I. Fachruddin,[1,*] Ch. Elster,[2] and W. Glöckle[1]
[1]*Institut für Theoretische Physik II, Ruhr-Universität Bochum, D-44780 Bochum, Germany*
[2]*Institut für Kernphysik, Forschungszentrum Jülich, D-52425 Jülich, Germany*
and Institute of Nuclear and Particle Physics, Ohio University, Athens, Ohio 45701
(Received 2 January 2001; published 18 April 2001)

A recently developed helicity basis for nucleon-nucleon (NN) scattering is applied to the deuteron bound state. Here the total spin of the deuteron is treated in such a helicity representation. For the bound state, two sets of two coupled eigenvalue equations are developed, where the amplitudes depend on two variables and one variable, respectively. Numerical illustrations based on the realistic Bonn-B NN potential are given. In addition, an ''operator form'' of the deuteron wave function is presented, and several momentum dependent spin densities are derived and shown, in which the angular dependence is given analytically.

DOI: 10.1103/PhysRevC.63.054003 PACS number(s): 13.75.Cs, 21.10.Hw, 21.45.+v, 27.10.+h

I. INTRODUCTION

In a recent paper [1] we developed a three-dimensional approach in momentum space for nucleon-nucleon (NN) scattering. The motivation is that for higher energies too many partial waves contribute and a direct solution seems more natural and economic. As relevant variables momentum vectors appear, specifically their magnitudes and the angles between them. The formulation in Ref. [1] is based on a helicity representation with respect to the total spin of the two nucleon system. This representation is different from the often used helicity basis referring to the individual nucleons [2,3]. A further important advantage of a three-dimensional approach is that a sometimes tedious partial wave expansion of a complex NN force is no longer needed. Instead one introduces a helicity representation of the NN force, which is perfectly adapted to the set of six operators completely describing the most general NN force compatible with general invariance principles. Thus, for any NN force given in operator form this scheme is applicable.

The helicity representation developed for NN scattering can also be applied to the bound NN system. It may appear unnecessary to extend this particular formulation to study the nonrelativistic deuteron, which only contains S and D waves. However, the standard practice requires a partial wave representation of the NN force, which we avoid. It is straightforward to extend the helicity formulation developed for scattering to investigate the deuteron, calculate its binding energy, and wave function properties. This is the purpose of the present investigation. In addition we study the various wave function properties in momentum space in a three-dimensional fashion. Our numerical example is based on the Bonn-B potential [4]. A graphical study of similar character has been carried out in configuration space [5] based on the AV18 nuclear force [6]. In addition we derive and display probability densities of various spin configurations for an overall polarized deuteron. These densities are based on analytical expressions, which we think are new.

In Sec. II we introduce the expansion of the deuteron state into helicity basis states as defined in Ref. [1]. Then we project the deuteron eigenvalue equation on these states. Since the deuteron has spin 1 there are three possible values for the helicity projections, namely, $\Lambda=1,0,-1$. Symmetry properties allow one to consider only $\Lambda=1,0$. Thus we obtain a set of two coupled equations in two variables, the magnitude $|\mathbf{q}|$ of the relative momentum vector and the angle between $\mathbf{q}$ and the arbitrarily chosen z axis. This two-dimensional form of the deuteron wave function is then connected to the standard partial wave representation. We demonstrate that this set of two coupled two-dimensional equations can be readily solved and display various wave function properties.

In Sec. III we derive the deuteron wave function in ''operator form.'' In a configuration space representation such a form has been given before [7]. For our purpose an operator form is an ideal starting point, since the spin degrees of freedom appear explicitly as spin operators, and thus fit perfectly into our helicity formulation. The projection of the wave function on the helicity basis leads to deuteron wave function components with an analytical angular behavior, which is different from the familiar one. The ''radial'' part of the wave function satisfies a set of two coupled ($\Lambda=1,0$), one-dimensional eigenvalue equations in $|\mathbf{q}|$. Based on this more analytical insight the connection to the standard S and D waves forms started in Sec. II can be finalized.

There are various possibilities that the two nucleons in the deuteron have a specific orientation of their spins for an overall polarized deuteron. For instance, both nucleons can have their spins up, or one nucleon can have its spin up and the other down. In Sec. IV we derive analytic expressions of the corresponding probabilities and display the results. This may have applications for electron scattering on the deuteron. Finally we summarize in Sec. V.

II. FORMULATION I

A. Deuteron wave function in the helicity basis

Let $|\Psi_d^{M_d}\rangle$ represent the deuteron state. Here M_d is the projection of the total angular momentum along a chosen

*Permanent address: Jurusan Fisika, FMIPA, Universitas Indonesia, Depok 16424, Indonesia.

axis, e.g., the z axis. The deuteron state will now be represented in the helicity basis $|\mathbf{q};\hat{q}S\Lambda;t\rangle^{\pi a}$ defined in Ref. [1]. Here $\mathbf{q}$ stands for the relative momentum of the two nucleons, S for the total spin, Λ for its projection along $\mathbf{q}$, and t for the total isospin. The index π denotes the parity of the state, and a indicates the state being antisymmetric. This results in

$$|\Psi_d^{M_d}\rangle=\frac{1}{4}\sum_{\Lambda=-1}^{1}\int d\mathbf{q}|\mathbf{q};\hat{q}1\Lambda;0\rangle^{1a\,1a}\langle\mathbf{q};\hat{q}1\Lambda;0|\Psi_d^{M_d}\rangle. \tag{2.1}$$

Here we took into account that for the deuteron $S=1,t=0$ and the parity is even. The general form of the helicity eigenstate is given by [1]

$$|\mathbf{q};\hat{q}S\Lambda;t\rangle^{\pi a}=(|\mathbf{q}\rangle+\eta_\pi|-\mathbf{q}\rangle)|\hat{q}S\Lambda\rangle|t\rangle, \tag{2.2}$$

where η_π denotes the parity eigenvalue. Using $|-\hat{q}S\Lambda\rangle=(-)^S|\hat{q}S-\Lambda\rangle$ one verifies the following properties:

$$\begin{aligned}|\mathbf{q};\hat{q}S\Lambda;t\rangle^{\pi a}&=\eta_\pi(-)^S(|-\mathbf{q}\rangle+\eta_\pi|\mathbf{q}\rangle)|-\hat{q}S-\Lambda\rangle|t\rangle\\&=\eta_\pi(-)^S|-\mathbf{q};-\hat{q}S-\Lambda;t\rangle^{\pi a}.\end{aligned} \tag{2.3}$$

With the above relations one obtains for the integral in Eq. (2.1)

$$\begin{aligned}&\int d\mathbf{q}|\mathbf{q};\hat{q}1-1;0\rangle^{1a\,1a}\langle\mathbf{q};\hat{q}1-1;0|\Psi_d^{M_d}\rangle\\&\quad=\int d\mathbf{q}\;|-\mathbf{q};-\hat{q}11;0\rangle^{1a\,1a}\langle-\mathbf{q};-\hat{q}11;0|\Psi_d^{M_d}\rangle\\&\quad=\int d\mathbf{q}|\mathbf{q};\hat{q}11;0\rangle^{1a\,1a}\langle\mathbf{q};\hat{q}11;0|\Psi_d^{M_d}\rangle.\end{aligned} \tag{2.4}$$

Hence, Eq. (2.1) simplifies to

$$\begin{aligned}|\Psi_d^{M_d}\rangle&=\int d\mathbf{q}\left\{\frac{1}{2}|\mathbf{q};\hat{q}11;0\rangle^{1a\,1a}\langle\mathbf{q};\hat{q}11;0|\Psi_d^{M_d}\rangle\right.\\&\quad\left.+\frac{1}{4}|\mathbf{q};\hat{q}10;0\rangle^{1a\,1a}\langle\mathbf{q};\hat{q}10;0|\Psi_d^{M_d}\rangle\right\}\\&\equiv\int d\mathbf{q}\left\{\frac{1}{2}|\mathbf{q};\hat{q}11;0\rangle^{1a}\varphi_1^{M_d}(\mathbf{q})\right.\\&\quad\left.+\frac{1}{4}|\mathbf{q};\hat{q}10;0\rangle^{1a}\varphi_0^{M_d}(\mathbf{q})\right\},\end{aligned} \tag{2.5}$$

where we defined

$$\varphi_\Lambda^{M_d}(\mathbf{q})\equiv{}^{1a}\langle\mathbf{q};\hat{q}1\Lambda;0|\Psi_d^{M_d}\rangle. \tag{2.6}$$

The azimuthal dependency of the amplitude defined in Eq. (2.6) can be found as follows. The state $|\mathbf{q};\hat{q}S\Lambda\rangle$ is obtained by rotating the state $|q\hat{z};\hat{z}S\Lambda\rangle$ from the z axis into the direction of $\mathbf{q}$ as

$$|\mathbf{q};\hat{q}S\Lambda\rangle=R(\hat{q})|q\hat{z};\hat{z}S\Lambda\rangle, \tag{2.7}$$

where $R(\hat{q})=\exp-iJ_z\phi\exp-iJ_y\theta$, and $\mathbf{J}=\mathbf{L}+\mathbf{S}$ is the operator of total angular momentum. It follows that

$$\begin{aligned}{}^{1a}\langle\mathbf{q};\hat{q}S\Lambda;t|\Psi_d^{M_d}\rangle&={}^{1a}\langle q\hat{z};\hat{z}S\Lambda;t|e^{iJ_y\theta}e^{iJ_z\phi}|\Psi_d^{M_d}\rangle\\&=e^{iM_d\phi}{}^{1a}\langle q\hat{z};\hat{z}S\Lambda;t|e^{iJ_y\theta}|\Psi_d^{M_d}\rangle.\end{aligned} \tag{2.8}$$

Thus, we can redefine $\varphi_\Lambda^{M_d}(\mathbf{q})$ such that the azimuthal dependency is factored out

$$\varphi_\Lambda^{M_d}(\mathbf{q})\equiv\varphi_\Lambda^{M_d}(q,\theta)e^{iM_d\phi}. \tag{2.9}$$

This leads to the final expression of the deuteron state in the helicity basis

$$\begin{aligned}|\Psi_d^{M_d}\rangle&=\int d\mathbf{q}\left\{\frac{1}{2}|\mathbf{q};\hat{q}11;0\rangle^{1a}\varphi_1^{M_d}(q,\theta)\right.\\&\quad\left.+\frac{1}{4}|\mathbf{q};\hat{q}10;0\rangle^{1a}\varphi_0^{M_d}(q,\theta)\right\}e^{iM_d\phi}.\end{aligned} \tag{2.10}$$

The normalization of the wave function components $\varphi_\Lambda^{M_d}(q,\theta)$ can be calculated as

$$\langle \Psi_d^{M_d}|\Psi_d^{M_d}\rangle = \int d\mathbf{q}' \int d\mathbf{q} \left\{ \frac{1}{2} {}^{1a}\langle \mathbf{q}';\hat{q}'11;0|\varphi_1^{M_d*}(q',\theta') + \frac{1}{4} {}^{1a}\langle \mathbf{q}';\hat{q}'10;0|\varphi_0^{M_d*}(q',\theta') \right\}$$
$$\times \left\{ \frac{1}{2}|\mathbf{q};\hat{q}11;0\rangle^{1a}\varphi_1^{M_d}(q,\theta) + \frac{1}{4}|\mathbf{q};\hat{q}10;0\rangle^{1a}\varphi_0^{M_d}(q,\theta) \right\}$$
$$= \int d\mathbf{q}' \int d\mathbf{q} \left\{ \frac{1}{4} {}^{1a}\langle \mathbf{q}';\hat{q}'11;0|\mathbf{q};\hat{q}11;0\rangle^{1a}\varphi_1^{M_d*}(q',\theta')\varphi_1^{M_d}(q,\theta) \right.$$
$$+ \frac{1}{16} {}^{1a}\langle \mathbf{q}';\hat{q}'10;0|.\mathbf{q};\hat{q}10;0\rangle^{1a}\varphi_0^{M_d*}(q',\theta')\varphi_0^{M_d}(q,\theta) + \frac{1}{8} {}^{1a}\langle \mathbf{q}';\hat{q}'11;0|\mathbf{q};\hat{q}10;0\rangle^{1a}\varphi_1^{M_d*}(q',\theta')\varphi_0^{M_d}(q,\theta)$$
$$\left. + \frac{1}{8} {}^{1a}\langle \mathbf{q}';\hat{q}'10;0|\mathbf{q};\hat{q}11;0\rangle^{1a}\varphi_0^{M_d*}(q',\theta')\varphi_1^{M_d}(q,\theta) \right\}$$
$$= 2\pi \int_0^\infty dq\, q^2 \int_{-1}^{1} d\cos\theta \left\{ \frac{1}{2}|\varphi_1^{M_d}(q,\theta)|^2 + \frac{1}{4}|\varphi_0^{M_d}(q,\theta)|^2 \right\}. \tag{2.11}$$

Here we used that

$${}^{\pi' a}\langle \mathbf{q}';\hat{q}'S'\Lambda';t'|\mathbf{q};\hat{q}S\Lambda;t\rangle^{\pi a} = [1-\eta_\pi(-)^{S+t}]\delta_{t't}\delta_{\eta_{\pi'}\eta_\pi}\delta_{S'S}[\delta(\mathbf{q}'-\mathbf{q})\delta_{\Lambda'\Lambda} + \eta_\pi(-)^S\delta(\mathbf{q}'+\mathbf{q})\delta_{\Lambda',-\Lambda}]. \tag{2.12}$$

From the normalization calculated using Eq. (2.1) we define a deuteron momentum density $\rho^{M_d}(\mathbf{q})$ as

$$\rho^{M_d}(\mathbf{q}) \equiv \frac{1}{4}|\varphi_1^{M_d}(\mathbf{q})|^2 + \frac{1}{4}|\varphi_0^{M_d}(\mathbf{q})|^2 + \frac{1}{4}|\varphi_1^{M_d}(-\mathbf{q})|^2 = \frac{1}{4}|\varphi_1^{M_d}(q,\theta)|^2 + \frac{1}{4}|\varphi_0^{M_d}(q,\theta)|^2 + \frac{1}{4}|\varphi_1^{M_d}(q,\pi-\theta)|^2. \tag{2.13}$$

B. The deuteron eigenvalue equation in the helicity basis

The deuteron state $|\Psi_d^{M_d}\rangle$ satisfies the eigenvalue equation

$$(H_0 - E_d + V)|\Psi_d^{M_d}\rangle = 0, \tag{2.14}$$

with E_d being the deuteron binding energy and V the NN potential. This eigenvalue equation is projected on the basis states $|\mathbf{q};\hat{q}1\Lambda;0\rangle^{1a}$ introduced in the previous section. Using Eq. (2.10) for representing $|\Psi_d^{M_d}\rangle$ one obtains

$${}^{1a}\langle \mathbf{q};\hat{q}1\Lambda;0|(H_0-E_d+V)|\Psi_d^{M_d}\rangle = {}^{1a}\langle \mathbf{q};\hat{q}1\Lambda;0|(H_0-E_d)|\Psi_d^{M_d}\rangle + {}^{1a}\langle \mathbf{q};\hat{q}1\Lambda;0|V\int d\mathbf{q}' \left\{ \frac{1}{2}|\mathbf{q}';\hat{q}'11;0\rangle^{1a}\varphi_1^{M_d}(q',\theta') \right.$$
$$\left. + \frac{1}{4}|\mathbf{q}';\hat{q}'10;0\rangle^{1a}\varphi_0^{M_d}(q',\theta') \right\} e^{iM_d\phi'}$$
$$= \left(\frac{q^2}{m} - E_d \right) \varphi_\Lambda^{M_d}(q,\theta)e^{iM_d\phi} + \frac{1}{2}\int d\mathbf{q}'\, {}^{1a}\langle \mathbf{q};\hat{q}1\Lambda;0|V|\mathbf{q}';\hat{q}'11;0\rangle^{1a}\varphi_1^{M_d}(q',\theta')e^{iM_d\phi'}$$
$$+ \frac{1}{4}\int d\mathbf{q}'\, {}^{1a}\langle \mathbf{q};\hat{q}1\Lambda;0|V|\mathbf{q}';\hat{q}'10;0\rangle^{1a}\varphi_0^{M_d}(q',\theta')e^{iM_d\phi'}$$
$$= \left(\frac{q^2}{m} - E_d \right) \varphi_\Lambda^{M_d}(q,\theta)e^{iM_d\phi} + \int d\mathbf{q}' \left\{ \frac{1}{2}V_{\Lambda 1}^{110}(\mathbf{q},\mathbf{q}')\varphi_1^{M_d}(q',\theta') \right.$$
$$\left. + \frac{1}{4}V_{\Lambda 0}^{110}(\mathbf{q},\mathbf{q}')\varphi_0^{M_d}(q',\theta') \right\} e^{iM_d\phi'}, \tag{2.15}$$

where $V^{\pi St}_{\Lambda\Lambda'}(\mathbf{q},\mathbf{q}') \equiv {}^{\pi a}\langle \mathbf{q};\hat{q}S\Lambda;t|V|\mathbf{q}';\hat{q}'S\Lambda';t\rangle^{\pi a}$. Thus, the eigenvalue equation for deuteron binding energy consists in the helicity basis of a set of two coupled integral equations

$$\left(\frac{q^2}{m}-E_d\right)\varphi^{M_d}_{\Lambda}(q,\theta) + \int d\mathbf{q}'\, e^{-iM_d(\phi-\phi')}\left\{\frac{1}{2}V^{110}_{\Lambda 1}(\mathbf{q},\mathbf{q}')\varphi^{M_d}_{1}(q',\theta') + \frac{1}{4}V^{110}_{\Lambda 0}(\mathbf{q},\mathbf{q}')\varphi^{M_d}_{0}(q',\theta')\right\}=0, \tag{2.16}$$

where the index Λ corresponds to 1 or 0. Since the wave function components $\varphi^{M_d}_{\Lambda}(q,\theta)$ have no azimuthal dependence, the ϕ' integral in Eq. (2.16) can be carried out independently. Defining

$$v^{\pi St,M_d}_{\Lambda\Lambda'}(q,q',\theta,\theta') \equiv \int_0^{2\pi} d\phi'\, e^{-iM_d(\phi-\phi')} V^{\pi St}_{\Lambda\Lambda'}(\mathbf{q},\mathbf{q}'), \tag{2.17}$$

the coupled integral equations are actually only two-dimensional and their final form reads

$$\left(\frac{q^2}{m}-E_d\right)\varphi^{M_d}_{\Lambda}(q,\theta) + \frac{1}{2}\int_0^{\infty} dq'\, q'^2 \int_{-1}^{1} d\cos\theta' \times v^{110,M_d}_{\Lambda 1}(q,q',\theta,\theta')\varphi^{M_d}_{1}(q',\theta') + \frac{1}{4}\int_0^{\infty} dq'\, q'^2 \int_{-1}^{1} d\cos\theta'\, v^{110,M_d}_{\Lambda 0}(q,q',\theta,\theta') \times \varphi^{M_d}_{0}(q',\theta')=0. \tag{2.18}$$

The eigenvalue equation, Eq. (2.18), is consistent with our treatment of the *NN* continuum of Ref. [1], where we derived coupled integral equations in two variables for the *NN* scattering equation. We would like to add the remark that it is not necessary to use any specific information about the the deuteron, namely, spin, isospin, and parity. The set of equations, Eq. (2.16), is valid for arbitrary S, η_π, and t. Any calculation based on a realistic *NN* potential will then reveal that a solution of the eigenvalue problem exists only for the well known quantum numbers. Therefore, the scheme laid out above automatically provides full insight, no *a priori* knowledge needs to be employed. At this level the question of total angular momentum of that bound state is undetermined and will be considered in Sec. III.

C. Partial wave projection of the deuteron wave function

In this subsection we want to relate $|\Psi^{M_d}_d\rangle$ as given in Eq. (2.10) to the standard partial wave representation of the deuteron. The standard representation of the total angular momentum basis $|q(lS)jm;t\rangle$ with the normalization

$$\langle q'(l'S')j'm'|q(lS)jm\rangle = \frac{\delta(q'-q)}{q'q}\delta_{l'l}\delta_{S'S}\delta_{j'j}\delta_{m'm} \tag{2.19}$$

is used for projecting the wave function $|\Psi^{M_d}_d\rangle$. Again, we use the fixed spin and isospin of the deuteron. The quantum numbers l, j, m remain arbitrary, and we obtain

$$\psi_l(q) \equiv \langle q(l1)jm;0|\Psi^{M_d}_d\rangle = \frac{1}{2}\int d\mathbf{q}'\langle q(l1)jm;0|\mathbf{q}';\hat{q}'11;0\rangle^{1a}\varphi^{M_d}_{1}(q',\theta') \times e^{iM_d\phi'} + \frac{1}{4}\int d\mathbf{q}'\langle q(l1)jm;0|\mathbf{q}';\hat{q}'10;0\rangle^{1a} \times \varphi^{M_d}_{0}(q',\theta')e^{iM_d\phi'}. \tag{2.20}$$

Recalling the explicit representation of the helicity state [1],

$$|\mathbf{q};\hat{q}S\Lambda\rangle = |\mathbf{q}\rangle|\hat{q}S\Lambda\rangle = \sum_{ljm}|q(lS)jm\rangle\sum_{\mu} C(lSj;\mu,m-\mu,m) \times Y^*_{l\mu}(\hat{q})e^{-i(m-\mu)\phi}d^S_{m-\mu,\Lambda}(\theta), \tag{2.21}$$

and using Eq. (2.2), the scalar product of partial wave and helicity basis can be worked out as

$$\langle q'(lS')jm;t'|\mathbf{q};\hat{q}S\Lambda;t\rangle^{\pi a}=(\langle q'(lS')jm|\mathbf{q}\rangle|\hat{q}S\Lambda\rangle+\eta_\pi\langle q'(lS')jm|-\mathbf{q}\rangle|\hat{q}S\Lambda\rangle)\langle t'|t\rangle$$

$$=\frac{\delta(q'-q)}{q'q}\delta_{S'S}\delta_{t't}\sum_\mu C(lSj;\mu,m-\mu,m)[Y^*_{l\mu}(\hat{q})+\eta_\pi Y^*_{l\mu}(-\hat{q})]e^{-i(m-\mu)\phi}d^S_{m-\mu,\Lambda}(\theta)$$

$$=[1+\eta_\pi(-)^l]\frac{\delta(q'-q)}{q'q}\delta_{S'S}\delta_{t't}\sum_\mu C(lSj;\mu,m-\mu,m)Y^*_{l\mu}(\hat{q})e^{-i(m-\mu)\phi}d^S_{m-\mu,\Lambda}(\theta)$$

$$=[1+\eta_\pi(-)^l]\sqrt{\frac{2l+1}{4\pi}}\frac{\delta(q'-q)}{q'q}\delta_{S'S}\delta_{t't}e^{-im\phi}\sum_\mu C(lSj;\mu,m-\mu,m)d^l_{\mu0}(\theta)d^S_{m-\mu,\Lambda}(\theta)$$

$$=[1+\eta_\pi(-)^l]\frac{\delta(q'-q)}{q'q}\delta_{S'S}\delta_{t't}\sqrt{\frac{2l+1}{4\pi}}e^{-im\phi}C(lSj;0\Lambda\Lambda)d^j_{m\Lambda}(\theta). \tag{2.22}$$

Here we used the relation

$$Y^*_{l\mu}(\hat{q})e^{i\mu\phi}=\sqrt{\frac{2l+1}{4\pi}}d^l_{\mu0}(\theta) \tag{2.23}$$

together with an addition theorem for Wigner's D functions

$$\sum_\mu C(lSj;\mu,m-\mu,m)d^l_{\mu0}(\theta)d^S_{m-\mu,\Lambda}(\theta)$$
$$=C(lSj;0\Lambda\Lambda)d^j_{m\Lambda}(\theta). \tag{2.24}$$

Hence, the projection of the deuteron state on the partial wave basis as defined in Eq. (2.20) is given by

$$\psi_l(q)=[1+(-)^l]\sqrt{\frac{2l+1}{4\pi}}\int_0^{2\pi}d\phi' e^{-i(m-M_d)\phi'}$$
$$\times\int_{-1}^1 d\cos\theta'\left\{\frac{1}{2}C(l1j;011)d^j_{m1}(\theta')\varphi_1^{M_d}(q,\theta')\right.$$
$$\left.+\frac{1}{4}C(l1j;000)d^j_{m0}(\theta')\varphi_0^{M_d}(q,\theta')\right\}$$
$$=[1+(-)^l]\sqrt{\pi(2l+1)}\delta_{mM_d}$$
$$\times\int_{-1}^1 d\cos\theta'\left\{\frac{1}{2}C(l1j;011)d^j_{m1}(\theta')\varphi_1^{M_d}(q,\theta')\right.$$
$$\left.+\frac{1}{4}C(l1j;000)d^j_{m0}(\theta')\varphi_0^{M_d}(q,\theta')\right\}. \tag{2.25}$$

This projection exists only for $m=M_d$ and even l, as enforced by the even deuteron parity, and one obtains

$$\psi_l(q)=2\sqrt{\pi(2l+1)}\int_{-1}^1 d\cos\theta'\left\{\frac{1}{2}C(l1j;011)d^j_{M_d1}(\theta')\right.$$
$$\left.\times\varphi_1^{M_d}(q,\theta')+\frac{1}{4}C(l1j;000)d^j_{M_d0}(\theta')\varphi_0^{M_d}(q,\theta')\right\}. \tag{2.26}$$

At this point the remaining properties for the projections $\psi_l(q)$ can be found by explicit calculation. In other words the fact that l has to be 0 and 2, and consequently $j=1$, has to be inferred numerically from the solution of Eq. (2.26). Of course an analytical investigation can be added once we adopt the deuteron wave function with the well-established analytical angular behavior (see Sec. III C).

D. Explicit solution of the deuteron eigenvalue equation

The numerical solution of the set of two coupled eigenvalue equations, Eq. (2.18), poses no specific difficulty. We employ an iterative, Lanczo's type technique [8,9], which provides both, eigenvalue and eigenvector. Following Ref. [10] the method is modified to avoid unphysical solutions corresponding to bound states in the repulsive core region. All numerical calculations are carried out with the Bonn-B potential [4].

For the discretization of Eq. (2.18) we employ Gaussian grids. The ϕ' integration over the potential, Eq. (2.17), needs only 10 quadrature points, whereas the $\cos\theta'$ integration requires at least 32 grid points and the q' integration 72 grid points, depending on the desired accuracy. The q' integration interval can safely be cut off at 30 fm^{-1}. Using these numerical parameters, we obtain the deuteron binding energy 2.224 MeV.

In Fig. 1 the two deuteron wave function components $\varphi_\Lambda^{M_d}(q,\theta)$, $\Lambda=0,1$, are shown for $M_d=0$ as functions of q and $\cos\theta$. Both drop quickly with increasing relative momentum between the two nucleons inside the deuteron. The wave function $\varphi_0^0(q,\theta)$ shows a cosinelike behavior indicated by the straight line at $q=0$ connecting the highest point at $\theta=0$ with the lowest point at $\theta=180°$ through zero at $\theta=90°$. This cosinelike behavior is confirmed to be true when considering the analytical angular behavior of the wave functions in Sec. III B. The function $\varphi_1^0(q,\theta)$, in contrast, displays a sinelike behavior, which also will prove to be its correct analytical form. It peaks at $\theta=90°$ and vanishes at $\theta=0$ and 180°. The maximum of $\varphi_0^0(q,\theta)$ is larger than that of $\varphi_1^0(q,\theta)$.

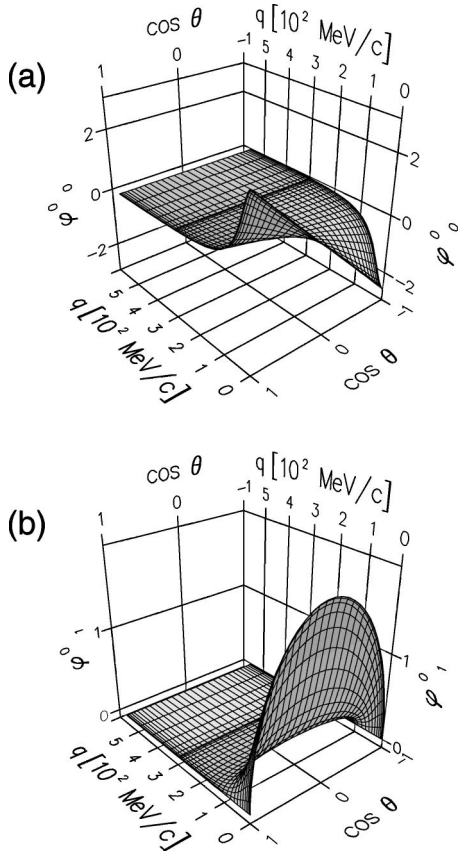

FIG. 1. The deuteron wave function components $\varphi_0^0(q,\theta)$ (a) and $\varphi_1^0(q,\theta)$ (b) in units 10^{-3} MeV$^{-1.5}$ as functions of q and $\cos\theta$.

For $M_d=1$ and -1 the wave function components $\varphi_\Lambda^{M_d}(q,\theta)$ are shown as functions of q and $\cos\theta$ in Fig. 2. They also drop quickly as the relative momentum between the two nucleons inside the deuteron increases. In the upper part of the figure we see that both $\varphi_0^1(q,\theta)$ and $\varphi_0^{-1}(q,\theta)$ vanish at $\theta=0$ and 180° but have a different sign for the other θ values. At $\theta=90°$ $\varphi_0^1(q,\theta)$ reaches its minimum whereas $\varphi_0^{-1}(q,\theta)$ reaches its maximum. In the lower part of the figure we see that $\varphi_1^1(q,\theta)$ peaks at $\theta=0$ and vanishes at $\theta=180°$. On the contrary $\varphi_1^{-1}(q,\theta)$ peaks at $\theta=180°$ and vanishes at $\theta=0$. This angular behavior of $\varphi_\Lambda^1(q,\theta)$ and $\varphi_\Lambda^{-1}(q,\theta)$ suggests a relation between the two functions. This relation is explicitly given in Sec. III B. For $M_d=1$ and -1 the maximum of $\varphi_1^{M_d}(q,\theta)$ is larger than that of $\varphi_0^{M_d}(q,\theta)$.

In Fig. 3 the deuteron densities $\rho^{M_d}(\mathbf{q})$ as given in Eq. (2.13) for $M_d=0$ (top row) and $M_d=1$ (bottom row) are shown. On the left side the two densities are displayed as functions of q and $\cos\theta$, and on the right side as functions of the Cartesian projections of $\mathbf{q}$, q_x, and q_z. Since the wave functions are invariant under rotations around the z axis, we show a vertical cut through the x-z plane. The densities $\rho^0(\mathbf{q})$ and $\rho^1(\mathbf{q})$ have uniform angular distributions with respect to the azimuthal angle θ for the momentum range shown, and thus the equidensity surfaces as function of the momentum between the two nucleons have a spherical shape. The densities are largest at small relative momentum $\mathbf{q}$. Though not shown here the deuteron density for $M_d=-1$ also has a similar shape. In Figs. 1–3 the densities have their maximum at $q=0$, indicating that the two nucleons being at rest with respect to each other is the most probable configuration for the deuteron.

Using Eq. (2.26) we extract the usual S and D wave components. They agree very well with the ones obtained from standard partial wave calculations.

III. FORMULATION II

A. Deuteron wave function in operator form

In order to study the different spin orientations of the two nucleons in the deuteron in relation to the vector of relative momentum a representation of the deuteron wave function in operator form is ideal. It is also desirable to derive another set of two coupled, one-dimensional equations, in the basis of total helicity.

In terms of the partial wave basis states given in Eq. (2.19) the deuteron state has the well-known form

$$|\Psi_d^{M_d}\rangle=|t\rangle\sum_{l=0,2}\int_0^\infty dq\,q^2|q(l1)1M_d\rangle\psi_l(q). \tag{3.1}$$

Here $|t\rangle$ indicates the isospin, which is 0 for the deuteron. The explicit reference to t will be omitted in the following considerations. Again, we would like to point out that we work in the basis of total helicity, and thus our final expressions will differ from the ones given in Ref. [3]. Carrying out the angular momentum expansion explicitly and using $\langle\hat{q}|l\mu\rangle=Y_{l\mu}(\hat{q})$ one obtains

$$\begin{aligned}\Psi_d^{M_d}(\mathbf{q})=&|1M_d\rangle\frac{1}{\sqrt{4\pi}}\psi_0(q)\\&+\{|11\rangle C(211;M_d-1,1M_d)Y_{2,M_d-1}(\hat{q})\\&+|10\rangle C(211;M_d0M_d)Y_{2M_d}(\hat{q})+|1-1\rangle\\&\times C(211;M_d+1,-1,M_d)Y_{2,M_d+1}(\hat{q})\}\psi_2(q).\end{aligned} \tag{3.2}$$

Inserting the explicit expressions for the Clebsch-Gordon coefficients [11] leads to

$$\begin{aligned}\Psi_d^{M_d}(\mathbf{q})=&|1M_d\rangle\frac{1}{\sqrt{4\pi}}\psi_0(q)\\&+\left\{|11\rangle\sqrt{\frac{(2-M_d)(3-M_d)}{20}}Y_{2,M_d-1}(\hat{q})\right.\\&-|10\rangle\sqrt{\frac{(2-M_d)(2+M_d)}{10}}Y_{2M_d}(\hat{q})\\&+|1-1\rangle\sqrt{\frac{(2+M_d)(3+M_d)}{20}}\\&\left.\times Y_{2,M_d+1}(\hat{q})\right\}\psi_2(q).\end{aligned} \tag{3.3}$$

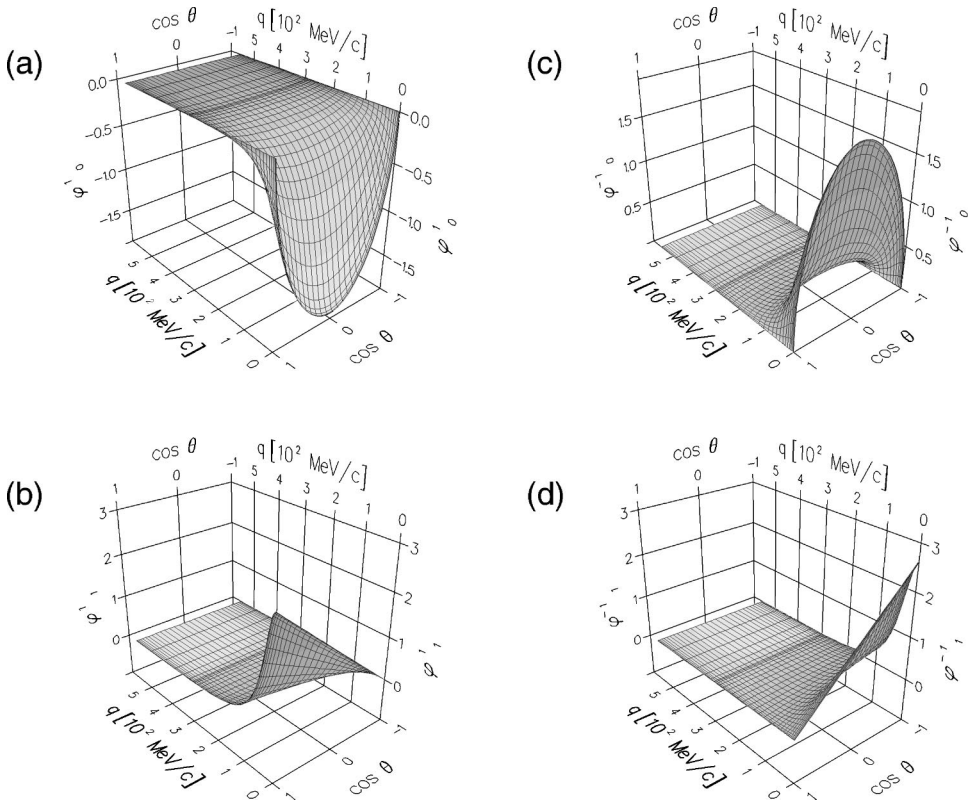

FIG. 2. The deuteron wave function components $\varphi_0^1(q,\theta)$ (a), $\varphi_1^1(q,\theta)$ (b), $\varphi_0^{-1}(q,\theta)$ (c), and $\varphi_1^{-1}(q,\theta)$ (d) in units 10^{-3} $\mathrm{MeV}^{-1.5}$ as functions of q and $\cos\theta$. The relation between the different components is discussed in Sec. II D.

Now we would like to express the wave function in a simple way such that

$$\Psi_d^{M_d}(\mathbf{q})=\{c_0\psi_0(q)+c_2\psi_2(q)\}|1M_d\rangle, \tag{3.4}$$

and where c_0 and c_2 are operators acting on the deuteron spin state $|1M_d\rangle$. For this purpose we choose as an example $M_d=1$ which yields

$$\begin{aligned}\Psi_d^1(\mathbf{q})&=|11\rangle\frac{1}{\sqrt{4\pi}}\psi_0(q)+\left\{|11\rangle\sqrt{\frac{1}{10}}Y_{20}(\hat{q})\right.\\&\left.-|10\rangle\sqrt{\frac{3}{10}}Y_{21}(\hat{q})+|1-1\rangle\sqrt{\frac{3}{5}}Y_{22}(\hat{q})\right\}\psi_2(q)\\&=|11\rangle\frac{1}{\sqrt{4\pi}}\psi_0(q)+\{|11\rangle(q_0^2+q_1q_{-1})-|10\rangle 3q_0q_1\\&+|1-1\rangle 3q_1^2\}\frac{1}{2q^2}\sqrt{\frac{1}{2\pi}}\psi_2(q).\end{aligned} \tag{3.5}$$

In the last step we expressed the spherical harmonic functions in terms of the spherical components of the momentum, q_1, q_0, and q_{-1} [11]. Since the state $|1M_d\rangle$ in Eq. (3.4) has already the correct transformation property under rotation of the deuteron state, the operators c_0 and c_2 must be scalars under rotation. Those scalars have to be formed out of the spherical components of $\boldsymbol{\sigma}(1)$ and $\boldsymbol{\sigma}(2)$ which at the same time will connect the given states $|1-1\rangle$, $|10\rangle$, and $|11\rangle$ to $|1M_d\rangle$. Therefore we consider

$$\begin{aligned}&\boldsymbol{\sigma}(1)\cdot\mathbf{q}\,\boldsymbol{\sigma}(2)\cdot\mathbf{q}|11\rangle\\&=[\sigma_0(1)q_0-\sigma_1(1)q_{-1}-\sigma_{-1}(1)q_1]\left|\frac{1}{2}\frac{1}{2}\right\rangle\\&\times[\sigma_0(2)q_0-\sigma_1(2)q_{-1}-\sigma_{-1}(2)q_1]\left|\frac{1}{2}\frac{1}{2}\right\rangle\\&=q_0^2|11\rangle-2q_0q_1|10\rangle+2q_1^2|1-1\rangle.\end{aligned} \tag{3.6}$$

The $l=0$ admixture can be projected out by subtracting $\frac{1}{3}q^2$, which leads to

$$\begin{aligned}\left(\boldsymbol{\sigma}(1)\cdot\mathbf{q}\,\boldsymbol{\sigma}(2)\cdot\mathbf{q}-\frac{1}{3}q^2\right)|11\rangle&=\frac{2}{3}(q_0^2+q_1q_{-1})|11\rangle\\&-2q_0q_1|10\rangle+2q_1^2|1-1\rangle.\end{aligned} \tag{3.7}$$

A comparison to the terms in Eq. (3.5) reveals that $\Psi_d^1(\mathbf{q})$ can be written as

$$\begin{aligned}\Psi_d^1(\mathbf{q})&=\left\{\frac{1}{\sqrt{4\pi}}\psi_0(q)+\left[\boldsymbol{\sigma}(1)\cdot\mathbf{q}\,\boldsymbol{\sigma}(2)\cdot\mathbf{q}\right.\right.\\&\left.\left.-\frac{1}{3}q^2\right]\frac{3}{4q^2}\sqrt{\frac{1}{2\pi}}\psi_2(q)\right\}|11\rangle\\&=\left\{\overline{\psi}_0(q)+\left[\boldsymbol{\sigma}(1)\cdot\mathbf{q}\,\boldsymbol{\sigma}(2)\cdot\mathbf{q}-\frac{1}{3}q^2\right]\overline{\psi}_2(q)\right\}|11\rangle,\end{aligned} \tag{3.8}$$

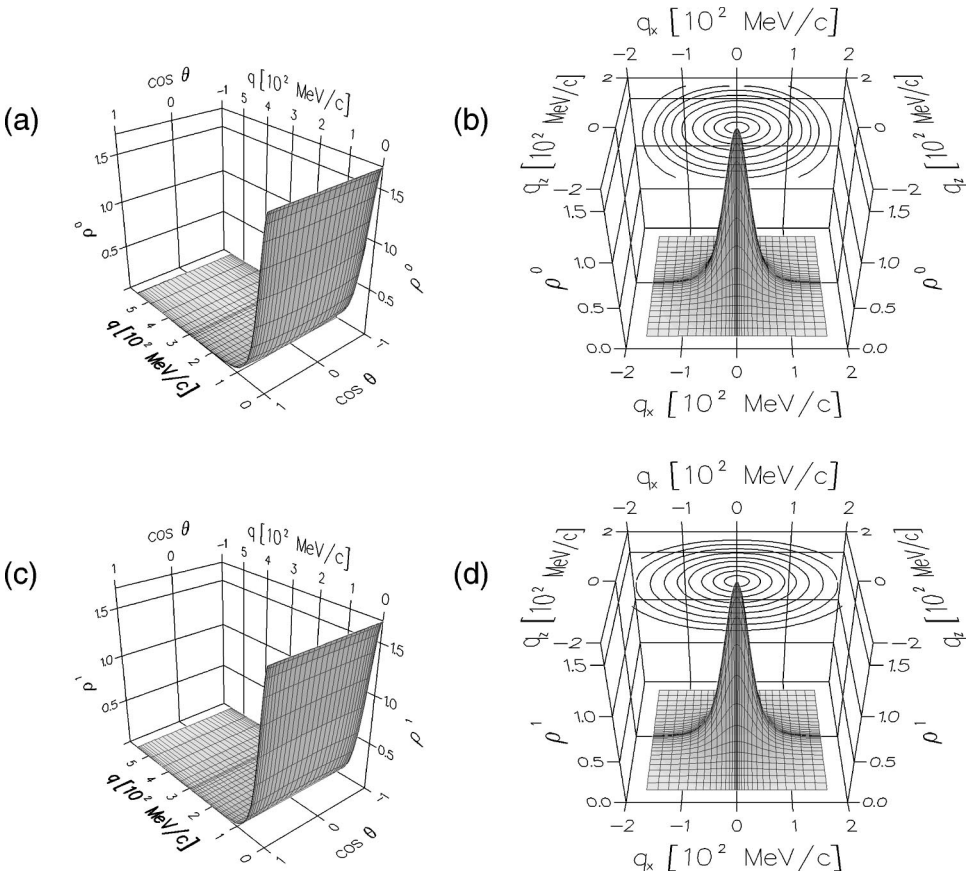

FIG. 3. The deuteron density for $M_d=0$ [(a) and (b)] and $M_d=1$ [(c) and (d)] in units 10^{-6} MeV^{-3} as functions of q and $\cos\theta$ [(a) and (c)] and as functions of q_x and q_z [(b) and (d)]. For the momentum range shown the deuteron densities display a uniform angular behavior. The contours represent equidensity lines along a vertical section in the x-z plane.

where

$$\overline{\psi}_0(q) \equiv \frac{1}{\sqrt{4\pi}}\psi_0(q), \tag{3.9}$$

$$\overline{\psi}_2(q) \equiv \frac{3}{4q^2}\frac{1}{\sqrt{2\pi}}\psi_2(q). \tag{3.10}$$

We denote the expression in Eq. (3.8) as ''operator form'' of the deuteron wave function in momentum space. A corresponding expression in coordinate space can be found in Ref. [7]. In a fashion similar to the above derivation, one can show that the form given in Eq. (3.8) is also valid for $M_d=0$ and -1. Hence, the deuteron wave function in operator form is given in momentum space as

$$\Psi_d^{M_d}(\mathbf{q}) = \left\{ \overline{\psi}_0(q) + \left[\boldsymbol{\sigma}(1)\cdot\mathbf{q}\,\boldsymbol{\sigma}(2)\cdot\mathbf{q} - \frac{1}{3}q^2 \right]\overline{\psi}_2(q) \right\} |1M_d\rangle. \tag{3.11}$$

Here the positive parity is manifest, since $\Psi_d^{M_d}(\mathbf{q}) = \Psi_d^{M_d}(-\mathbf{q})$. It is a straightforward algebra to work out the normalization of $|\Psi_d^{M_d}\rangle$ as given in Eq. (3.11) and one obtains

$$\begin{aligned}\langle \Psi_d^{M_d} | \Psi_d^{M_d} \rangle &= \int d\mathbf{q} \langle 1M_d | \left\{ \overline{\psi}_0(q) + \left[\boldsymbol{\sigma}(1)\cdot\mathbf{q}\,\boldsymbol{\sigma}(2)\cdot\mathbf{q} - \frac{1}{3}q^2 \right]\overline{\psi}_2(q) \right\} \left\{ \overline{\psi}_0(q) + \left[\boldsymbol{\sigma}(1)\cdot\mathbf{q}\,\boldsymbol{\sigma}(2)\cdot\mathbf{q} - \frac{1}{3}q^2 \right]\overline{\psi}_2(q) \right\} |1M_d\rangle \\ &= 4\pi \int_0^\infty dq\, q^2 \left\{ \overline{\psi}_0^2(q) + \frac{8}{9}q^4 \overline{\psi}_2^2(q) \right\} \\ &= \int_0^\infty dq\, q^2 \{ \psi_0^2(q) + \psi_2^2(q) \}. \end{aligned} \tag{3.12}$$

The last form is the standard normalization of the deuteron wave function in terms of partial wave components. In arriving at this result we used that

$$\langle 1M_d | \boldsymbol{\sigma}(1)\cdot\mathbf{q}\,\boldsymbol{\sigma}(2)\cdot\mathbf{q} | 1M_d \rangle = \begin{cases} q_0^2, & M_d = \pm 1, \\ q^2 - 2q_0^2, & M_d = 0, \end{cases} \tag{3.13}$$

and

$$\int d\hat{q}\, \langle 1M_d | \boldsymbol{\sigma}(1)\cdot\mathbf{q}\,\boldsymbol{\sigma}(2)\cdot\mathbf{q} | 1M_d \rangle = \frac{4\pi}{3}q^2. \tag{3.14}$$

As we shall show in Sec. IV based on the form given in Eq. (3.11) one can express the angular dependencies of all possible spin orientations in the deuteron analytically.

B. Analytical angular behavior of the deuteron wave function and the deuteron eigenvalue equation

With the operator form, Eq. (3.11), at hand we revisit the deuteron wave function component in the helicity basis as given in Eq. (2.6):

$$\begin{aligned}\varphi_{\Lambda}^{M_d}(\mathbf{q}) &\equiv {}^{1a}\langle \mathbf{q};\hat{q}1\Lambda;0|\Psi_d^{M_d}\rangle \\ &= \langle \hat{q}1\Lambda|(\langle \mathbf{q}| + \langle -\mathbf{q}|)\Psi_d^{M_d}\rangle \\ &= 2\langle \hat{q}1\Lambda|\Psi_d^{M_d}(\mathbf{q}) \\ &= 2\langle \hat{q}1\Lambda|\Bigg\{ \overline{\psi}_0(q) \\ &\quad + \left[\boldsymbol{\sigma}(1)\cdot\mathbf{q}\,\boldsymbol{\sigma}(2)\cdot\mathbf{q} - \frac{1}{3}q^2 \right]\overline{\psi}_2(q)\Bigg\}|1M_d\rangle. \end{aligned} \tag{3.15}$$

The operator $\boldsymbol{\sigma}(1)\cdot\mathbf{q}\,\boldsymbol{\sigma}(2)\cdot\mathbf{q}$ can be expressed in terms of the total helicity $\mathbf{S}\cdot\mathbf{q}$ as

$$\boldsymbol{\sigma}(1)\cdot\mathbf{q}\,\boldsymbol{\sigma}(2)\cdot\mathbf{q} = 2(\mathbf{S}\cdot\mathbf{q})^2 - q^2, \tag{3.16}$$

where $\mathbf{S}=\frac{1}{2}[\boldsymbol{\sigma}(1)+\boldsymbol{\sigma}(2)]$. Therefore, the helicity wave function component is given by

$$\begin{aligned}\varphi_{\Lambda}^{M_d}(\mathbf{q}) &= 2\langle \hat{q}1\Lambda|\left\{ \overline{\psi}_0(q) + \left[2(\mathbf{S}\cdot\mathbf{q})^2 - \frac{4}{3}q^2 \right]\overline{\psi}_2(q)\right\}|1M_d\rangle \\ &= 2\left\{ \overline{\psi}_0(q) + \left[2\Lambda^2 - \frac{4}{3}\right]q^2\overline{\psi}_2(q)\right\}\langle \hat{q}1\Lambda|1M_d\rangle \\ &= 2\left\{ \overline{\psi}_0(q) + \left[2\Lambda^2 - \frac{4}{3}\right]q^2\overline{\psi}_2(q)\right\} D^{1*}_{M_d\Lambda}(\phi\theta 0) \\ &= 2\left\{ \overline{\psi}_0(q) + \left[2\Lambda^2 - \frac{4}{3}\right]q^2\overline{\psi}_2(q)\right\} e^{iM_d\phi} d^1_{M_d\Lambda}(\theta). \end{aligned} \tag{3.17}$$

This shows that the angular behavior of the wave function component is given by $e^{iM_d\phi}d^1_{M_d\Lambda}(\theta)$, where the d matrix is explicitly given as [11]

$$d^1_{M_d\Lambda}(\theta) = \begin{pmatrix} \frac{1+\cos\theta}{2} & -\frac{\sin\theta}{\sqrt{2}} & \frac{1-\cos\theta}{2} \\ \frac{\sin\theta}{\sqrt{2}} & \cos\theta & -\frac{\sin\theta}{\sqrt{2}} \\ \frac{1-\cos\theta}{2} & \frac{\sin\theta}{\sqrt{2}} & \frac{1+\cos\theta}{2} \end{pmatrix}. \tag{3.18}$$

Finally, we define an angle independent function $\Phi_\Lambda(q)$ via

$$\begin{aligned}\Phi_\Lambda(q) &\equiv \overline{\psi}_0(q) + \left[2\Lambda^2 - \frac{4}{3}\right]q^2\overline{\psi}_2(q) \\ &= \frac{1}{\sqrt{4\pi}}\psi_0(q) + [3\Lambda^2 - 2]\frac{1}{\sqrt{8\pi}}\psi_2(q), \end{aligned} \tag{3.19}$$

so that the deuteron wave function component can be expressed as

$$\begin{aligned}\varphi_{\Lambda}^{M_d}(\mathbf{q}) &= 2\Phi_\Lambda(q)e^{iM_d\phi}d^1_{M_d\Lambda}(\theta) \\ &\equiv \varphi_{\Lambda}^{M_d}(q,\theta)e^{iM_d\phi}. \end{aligned} \tag{3.20}$$

Here $\varphi_{\Lambda}^{M_d}(q,\theta)$ are the wave function components which we determined previously numerically and which are displayed in Figs. 1 and 2.

Employing the above given form of the deuteron wave function, we can derive a one-dimensional eigenvalue equation, starting from the eigenvalue equation for $\varphi_{\Lambda}^{M_d}(q,\theta) = \varphi_{\Lambda}^{M_d}(\mathbf{q})\exp(-iM_d\phi)$. Inserting Eq. (3.20) into Eq. (2.16) gives

$$\begin{aligned}&\left(\frac{q^2}{m} - E_d\right)\Phi_\Lambda(q)d^1_{M_d\Lambda}(\theta) \\ &\quad + \int d\mathbf{q}'\, e^{-iM_d(\phi-\phi')}\Bigg\{ \frac{1}{2}V^{110}_{\Lambda 1}(\mathbf{q},\mathbf{q}')\Phi_1(q')d^1_{M_d 1}(\theta') \\ &\quad + \frac{1}{4}V^{110}_{\Lambda 0}(\mathbf{q},\mathbf{q}')\Phi_0(q')d^1_{M_d 0}(\theta')\Bigg\} = 0, \end{aligned} \tag{3.21}$$

an equation which is valid for any direction θ. Choosing $\hat{q} = \hat{z}$ simplifies the equation, since the azimuthal dependencies of the potential can be factored out as

$$V^{\pi St}_{\Lambda\Lambda'}(q\hat{z},\mathbf{q}') \equiv e^{i\Lambda(\phi-\phi')}V^{\pi St}_{\Lambda\Lambda'}(q,q',\theta'). \tag{3.22}$$

The d matrix in the first term gives $\delta_{M_d\Lambda}$, and the ϕ' integration requires Λ to be equal M_d, leading to

$$\left(\frac{q^2}{m} - E_d\right)\Phi_{M_d}(q) + \pi\int_0^\infty dq'\, q'^2\int_{-1}^{1} d\cos\theta'\left\{ V^{110}_{M_d 1}(q,q',\theta')\Phi_1(q')d^1_{M_d 1}(\theta') + \frac{1}{2}V^{110}_{M_d 0}(q,q',\theta')\Phi_0(q')d^1_{M_d 0}(\theta')\right\} = 0. \tag{3.23}$$

Choosing $M_d=1$ and 0 leads to a closed system of two coupled equations for the amplitudes Φ_1 and Φ_0. The $\cos\theta'$ integration can be worked out independent of the amplitudes $\Phi_\Lambda(q')$, so that Eq. (3.23) is in fact a set of two coupled equations in one variable, namely, q

$$\left(\frac{q^2}{m}-E_d\right)\Phi_{M_d}(q)+\pi\int_0^\infty dq'\,q'^2\left\{V^{110}_{M_d1}(q,q')\Phi_1(q')+\frac{1}{2}V^{110}_{M_d0}(q,q')\Phi_0(q')\right\}=0, \tag{3.24}$$

with

$$V^{110}_{M_d\Lambda'}(q,q')\equiv\int_{-1}^{1}d\cos\theta'\,V^{110}_{M_d\Lambda'}(q,q',\theta')d^1_{M_d\Lambda'}(\theta'). \tag{3.25}$$

The set of two coupled eigenvalue equations (3.24) can be easily solved using the same method as described in Sec. II D. The Gaussian grids for the q' integration and the $\cos\theta'$ integration in Eq. (3.25) are taken to be the same, and we obtain the same value for the deuteron binding energy, $E_d=2.224$ MeV. The solutions $\Phi_0(q)$ and $\Phi_1(q)$ are displayed in Fig. 4. This figure shows that both functions are of the same magnitude for $q=0$, and both drop by about one order of magnitude within q of $\approx$200 MeV/c. $\Phi_1(q)$ has its first node already for $q\approx300$ MeV/c, while the first node of $\Phi_0(q)$ occurs for $q\approx800$ MeV/c. In general, the magnitude of $\Phi_0(q)$ falls off slightly slower than the one for $\Phi_1(q)$ as a function of q.

In Figs. 1 and 2 the wave function components $\varphi^{M_d}_\Lambda(q,\theta)$ are obtained from numerically solving Eq. (2.18). With the help of Eqs. (3.20) and (3.18) we can express their angular behavior as

$$M_d=0:\varphi^0_0(q,\theta)=2\Phi_0(q)\cos\theta, \tag{3.26}$$

$$\varphi^0_1(q,\theta)=\sqrt{2}\Phi_1(q)\sin\theta, \tag{3.27}$$

$$M_d=1:\varphi^1_0(q,\theta)=-\sqrt{2}\Phi_0(q)\sin\theta, \tag{3.28}$$

$$\varphi^1_1(q,\theta)=\Phi_1(q)(1+\cos\theta). \tag{3.29}$$

Obviously, the angular behavior extracted numerically agrees with the analytical one.

We mentioned in Sec. II D that the maximum of $\varphi^{M_d}_\Lambda(q,\theta)$ with $\Lambda=M_d$ is larger than that with $\Lambda\neq M_d$. Equations (3.26)–(3.29) show that the ratio $|\varphi^{M_d}_{M_d}(q,\theta)_{\max}/\varphi^{M_d}_{\Lambda\neq M_d}(q,\theta)_{\max}|$ is exactly $\sqrt{2}$. This can be understood as follows. According to Eq. (3.19) the component $\varphi^{M_d}_\Lambda(q,\theta)$ is determined for small q dominantly by $\psi_0(q)$, i.e., the S wave.

The analytical angular behavior of the deuteron densities given in Eq. (2.13) can now easily be derived. For $M_d=0,1$ we find

$$\rho^0(\mathbf{q})=\Phi_1^2(q)\sin^2\theta+\Phi_0^2(q)\cos^2\theta, \tag{3.30}$$

$$\rho^1(\mathbf{q})=\frac{1}{2}\Phi_1^2(q)(1+\cos^2\theta)+\frac{1}{2}\Phi_0^2(q)\sin^2\theta. \tag{3.31}$$

From these expressions we can deduce that $\rho^0(\mathbf{q})$ and $\rho^1(\mathbf{q})$ are only perfect spheres for small q, where $\Phi_0(q)$ and $\Phi_1(q)$ are almost identical. For larger momenta the spheres are deformed according the ratio $|\Phi_0(q)/\Phi_1(q)|$.

C. Relation to the conventional partial wave representation

Before completing the considerations about the analytic behavior of the angular behavior of the deuteron wave function in the helicity basis, we want to make contact with the standard representation of the deuteron wave function. In Sec. II C we derived the projection of the deuteron state on the partial wave basis. We ended up with Eq. (2.26) and left the remaining quantum numbers j and l to be determined numerically. The wave function components $\varphi_\Lambda(q,\theta)$ together with their analytical angle behavior allows to calculate the projection and to determine the remaining conditions for their existence. Inserting Eq. (3.20) into Eq. (2.26) yields

$$\psi_l(q)=2\sqrt{\pi(2l+1)}\int_{-1}^{1}d\cos\theta'\left\{C(l1j;011)d^j_{M_d1}(\theta')\Phi_1(q)d^1_{M_d1}(\theta')+\frac{1}{2}C(l1j;000)d^j_{M_d0}(\theta')\Phi_0(q)d^1_{M_d0}(\theta')\right\}$$
$$=\frac{4}{3}\delta_{j1}\sqrt{\pi(2l+1)}\left\{C(l1j;011)\Phi_1(q)+\frac{1}{2}C(l1j;000)\Phi_0(q)\right\}. \tag{3.32}$$

Here we use the orthogonality property of the d matrix

$$\int_{-1}^{1}d\cos\theta\,d^{j_1}_{\mu_1m_1}(\theta)d^{j_2}_{\mu_2m_2}(\theta)=\frac{2}{2j_1+1}\delta_{j_1j_2}\delta_{\mu_1\mu_2}\delta_{m_1m_2}. \tag{3.33}$$

The projection exists only for a total angular momentum $j=1$. Furthermore, the Clebsch-Gordan coefficients allow only $l=0$ and $l=2$ and we obtain explicitly for the S and D wave

$$\psi_0(q)=\frac{2}{3}\sqrt{\pi}\{2\Phi_1(q)+\Phi_0(q)\}, \tag{3.34}$$

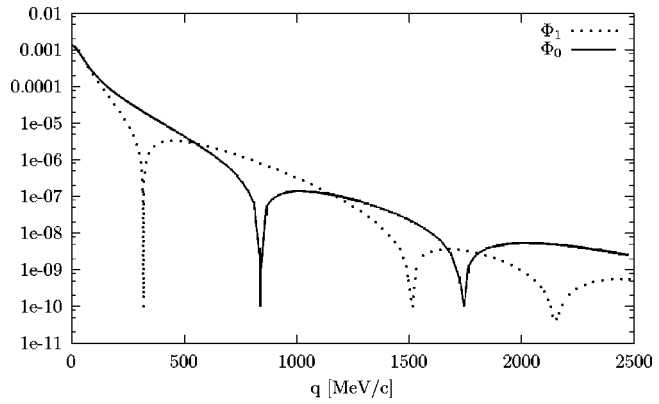

FIG. 4. The wave functions $|\Phi_0(q)|$ and $|\Phi_1(q)|$ in units $\mathrm{MeV}^{-1.5}$.

$$\psi_2(q)=\frac{2}{3}\sqrt{2\pi}\{\Phi_1(q)-\Phi_0(q)\}, \tag{3.35}$$

which is consistent with Eq. (3.19). We extracted the *S* and *D* waves from Eqs. (3.34) and (3.35) and found to be in very good agreement with the ones obtained from a standard partial wave solution of the deuteron eigenvalue problem.

IV. PROBABILITY DENSITIES FOR DIFFERENT SPIN CONFIGURATIONS

The operator form of the deuteron wave function given in Eq. (3.11) is an ideal tool to express probabilities for different spin configurations within the deuteron. This provides analytical insight into the shape of these configurations. As an example we choose a polarized deuteron with $M_d=1$. Cases of interest are if (1) both nucleons have their spins up, (2) both nucleons have their spins down, (3) one nucleon has spin up and the other has spin down, (4) one nucleon has spin up and the other has arbitrary spin orientation, and (5) one nucleon has spin down and the other has arbitrary spin orientation. For these five cases the probability densities are given below. For clarity the final expressions are given in terms of the standard *S* and *D* waves.

(1) Probability density for both nucleons having their spins up:

$$\rho^1_{\uparrow\uparrow}(\mathbf{q})\equiv\Psi^1_d{}^*(\mathbf{q})\frac{1}{2}[1+\sigma_z(1)]\frac{1}{2}[1+\sigma_z(2)]\Psi^1_d(\mathbf{q})$$
$$=\frac{1}{4\pi}\left\{\psi_0^2(q)+\frac{3}{\sqrt{2}}\left(\cos^2\theta-\frac{1}{3}\right)\psi_0(q)\psi_2(q)\right.$$
$$\left.+\frac{9}{8}\left(\cos^2\theta-\frac{1}{3}\right)^2\psi_2^2(q)\right\}. \tag{4.1}$$

(2) Probability density for both nucleons having their spins down:

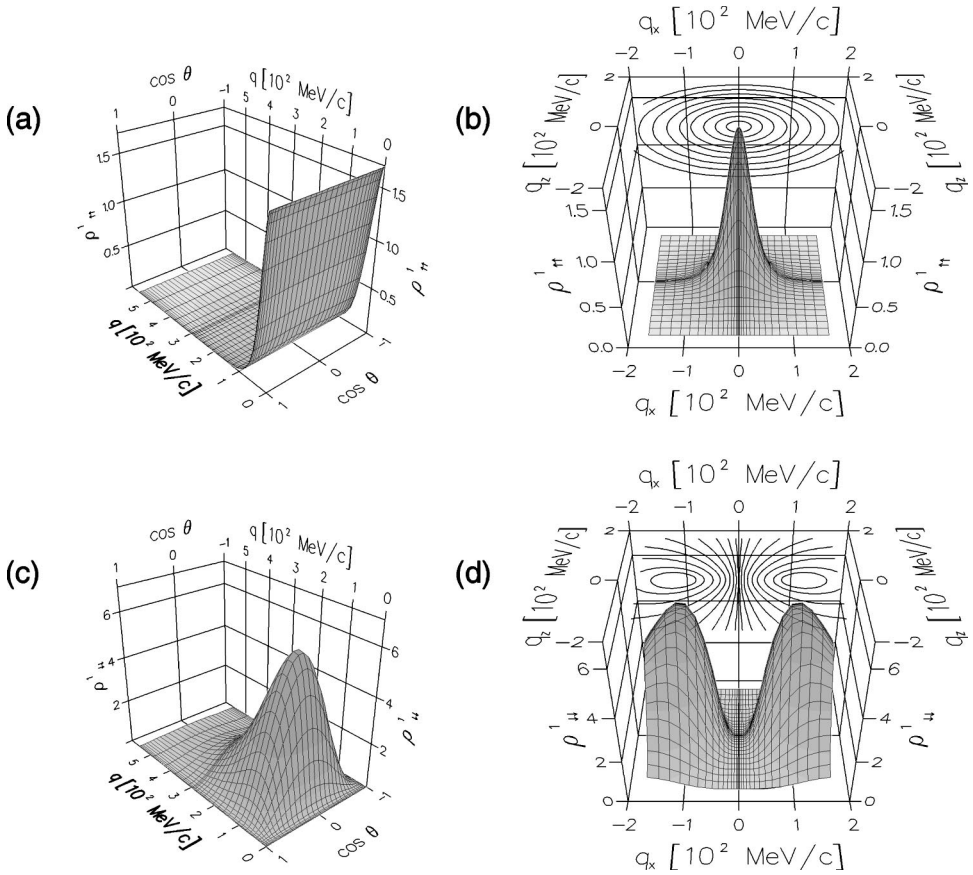

FIG. 5. The probability densities $\rho^1_{\uparrow\uparrow}(\mathbf{q})$ in units 10^{-6} MeV^{-3} for both nucleons having their spins up [(a) and (b)] and $\rho^1_{\downarrow\downarrow}(\mathbf{q})$ in units 10^{-10} MeV^{-3} for both nucleons having their spins down [(c) and (d)]. The contours represent equidensity lines along a vertical section in the *x*-*z* plane.

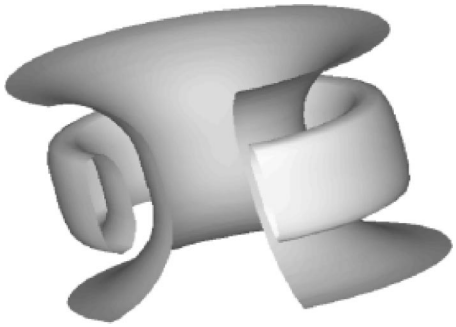

FIG. 6. Two selected equidensity surfaces of the probability density $\rho^1_{\downarrow\downarrow}(\mathbf{q})$ for both nucleons having their spins down. The image is created by rotating two of the equidensity lines of Fig. 5(d) around the z axis. Note that the z axis is stretched with respect to the other two axes.

$$\rho^1_{\downarrow\downarrow}(\mathbf{q}) \equiv \Psi^{1\,*}_d(\mathbf{q}) \frac{1}{2}[1-\sigma_z(1)] \frac{1}{2}[1-\sigma_z(2)] \Psi^1_d(\mathbf{q})$$
$$= \frac{9}{32\pi} \sin^4\theta \;\; \psi_2^2(q). \tag{4.2}$$

(3) Probability density for one nucleon having spin up and the other having spin down:

$$\rho^1_{\uparrow\downarrow}(\mathbf{q}) \equiv \Psi^{1\,*}_d(\mathbf{q}) \frac{1}{2}[1+\sigma_z(1)] \frac{1}{2}[1-\sigma_z(2)] \Psi^1_d(\mathbf{q})$$
$$= \frac{9}{32\pi} \cos^2\theta \sin^2\theta \;\; \psi_2^2(q). \tag{4.3}$$

(4) Probability density for one nucleon having spin up and the other having arbitrary spin orientation:

$$\rho^1_{\uparrow(1)}(\mathbf{q}) \equiv \Psi^{1\,*}_d(\mathbf{q}) \frac{1}{2}[1+\sigma_z(1)] \Psi^1_d(\mathbf{q})$$
$$= \frac{1}{4\pi}\left[\psi_0^2(q) + \frac{3}{\sqrt{2}}\left(\cos^2\theta - \frac{1}{3}\right) \psi_0(q)\psi_2(q) + \frac{9}{8}\left\{ \left(\cos^2\theta - \frac{1}{3}\right)^2 + \cos^2\theta \sin^2\theta \right\} \psi_2^2(q) \right]$$
$$= \rho^1_{\uparrow\uparrow}(\mathbf{q}) + \rho^1_{\uparrow\downarrow}(\mathbf{q}). \tag{4.4}$$

(5) Probability density for one nucleon having spin down and the other having arbitrary spin orientation:

$$\rho^1_{\downarrow(1)}(\mathbf{q}) \equiv \Psi^{1\,*}_d(\mathbf{q}) \frac{1}{2}[1-\sigma_z(1)] \Psi^1_d(\mathbf{q})$$
$$= \frac{9}{32\pi} \sin^2\theta \psi_2^2(q)$$
$$= \rho^1_{\uparrow\downarrow}(\mathbf{q}) + \rho^1_{\downarrow\downarrow}(\mathbf{q}). \tag{4.5}$$

In Figs. 5–9 those five different probability densities are shown. In each figure the left side displays the probability densities as functions of q and $\cos\theta$, whereas the right side depicts the probability densities as functions of q_x and q_z. The contour lines represent a vertical section in the x-z plane through equidensity surfaces. Rotating this section around the q_z axis gives a three-dimensional image of the equidensity surfaces.

The probability densities for the first two cases, where both nucleons have the same spin orientations, are given in Fig. 5. The top row represents $\rho^1_{\uparrow\uparrow}(\mathbf{q})$. The density peaks at $\mathbf{q}=0$, indicating that the largest densities occur at small momenta. This density has a spherical shape, since Eq. (4.1) is dominated by the S wave, and in the momentum range shown has little dependence on the angle θ. The figures in the bottom row represent $\rho^1_{\downarrow\downarrow}(\mathbf{q})$. As Eq. (4.2) suggests, this density is only determined by the deuteron D wave times a function of the angle θ. Thus at $\mathbf{q}=0$ it is zero, and reaches two maxima at $|q_{\max}| \approx 100$ MeV/c along the q_x axis ($\theta = \pi/2$). If a measurement could be carried out on a deuteron at rest the two nucleons would have momenta back to back

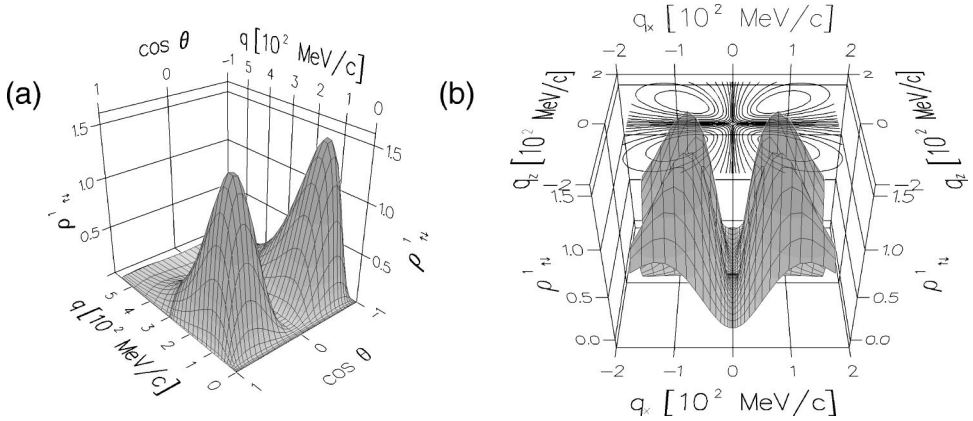

FIG. 7. The probability density $\rho^1_{\uparrow\downarrow}(\mathbf{q})$ in units 10^{-10} MeV^{-3} for one nucleon having spin up and the other having spin down. The contours represent equidensity lines along a vertical section in the x-z plane.

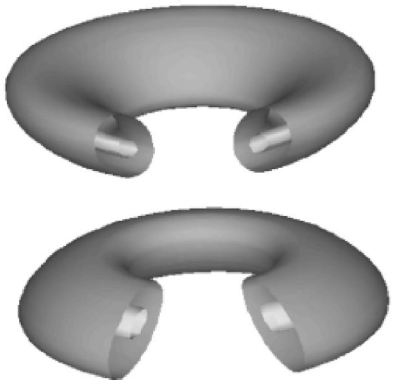

FIG. 8. Two selected equidensity surfaces of the probability density $\rho^1_{\uparrow\downarrow}(\mathbf{q})$ for one nucleon having spin up and the other having spin down. The image is created by rotating two of the equidensity lines of Fig. 7(b) around the z axis.

perpendicular to the polarization axis of the deuteron. Rotating the vertical section given in Fig. 5(d) around the z axis will show a toroidal shape of the equidensity surfaces of the probability density in this configuration. For the image in Fig. 6, two equidensity surfaces, one with a high value, being closed in the section of Fig. 5(d), and one with a small value are picked and rotated around the z axis resulting in a torus, being cut open vertically. The surface of lower density is left half open at the outer side. The image displays a shape characteristic for the spherical harmonics with $l=2$, $m=2$.

For the case where the spins of the two nucleons point in opposite directions, the probability density is shown in Fig. 7. According to Eq. (4.3), this density is also given solely by the deuteron D wave and a function of the angle θ. It has four peaks of equal height in each quadrant of the q_x-q_z plane at $|q_x|=|q_z|=q_{\max}\cos(\pi/4)$. Rotating the vertical section in the x-z plane around the z axis will reveal a double toroidal structure. For the image in Fig. 8 two equidensity surfaces are picked and rotated around the z axis, resulting in a double torus being cut open vertically. The inner tubes represent surfaces of higher density compared to the outer ones. The shape is characteristic for a spherical harmonics with $l=2$, $m=1$. Again, a measurement on the deuteron at rest would see in the maxima the two nucleons with momenta back to back pointing at $\theta=45°$.

For the remaining two cases given by Eqs. (4.4) and (4.5), where only one of the two nucleons is polarized, the probability densities are presented in Fig. 9. The figures in the top row represent $\rho^1_{\uparrow(1)}(\mathbf{q})$. For the momentum range shown its properties are very similar to $\rho^1_{\uparrow\uparrow}(\mathbf{q})$ given in the top row of Fig. 5. The reason is that $\rho^1_{\uparrow\uparrow}(\mathbf{q})$ is larger than $\rho^1_{\uparrow\downarrow}(\mathbf{q})$ and thus dominates. The figures in the bottom row depict $\rho^1_{\downarrow(1)}(\mathbf{q})$. This density has the same maxima as $\rho^1_{\downarrow\downarrow}(\mathbf{q})$ given in Fig. 5(d), but a slightly different angular behavior. For a fixed q the changes with θ are slower than for $\rho^1_{\downarrow\downarrow}(\mathbf{q})$. This is caused by the linear dependence on $\sin^2\theta$, whereas $\rho^1_{\downarrow\downarrow}(\mathbf{q})$ has a quadratic one.

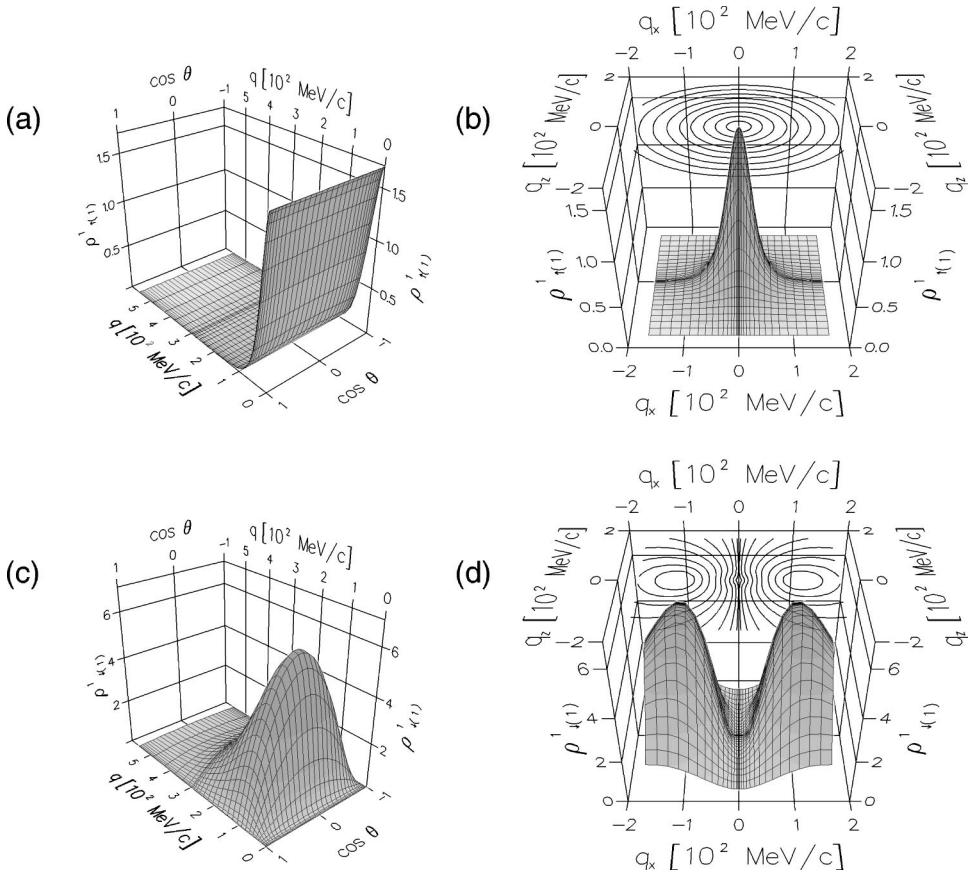

FIG. 9. The probability densities $\rho^1_{\uparrow(1)}(\mathbf{q})$ in units 10^{-6} MeV^{-3} for one nucleon having spin up whereas the other having arbitrary spin orientation [(a) and (b)] and $\rho^1_{\downarrow(1)}(\mathbf{q})$ in units 10^{-10} MeV^{-3} for one nucleon having spin down whereas the other having arbitrary spin orientation [(c) and (d)]. The contours represent equidensity lines along a vertical section in the x-z plane.

V. SUMMARY

As an object with internal structure it is tempting to investigate the deuteron properties three dimensionally. To that aim we study the deuteron properties in a representation based on the total helicity of the two-body system taken along the relative momentum of the two particles. Though originally developed for describing *NN* scattering, the method is general and can be used to solve bound state problems as well.

We introduce deuteron wave function components in the helicity basis. They depend on the magnitude q of the relative momentum and the angle θ of the relative momentum $\mathbf{q}$ to the z axis. Deriving an ''operator form'' of the deuteron wave function one obtains insight into the analytical angular behavior of those components.

We derived two sets of two coupled eigenvalue equations for deuteron wave functions. The first set of equations does not use any *a priori* knowledge of the quantum numbers of the deuteron, and the *NN* potential representation in helicity basis is used similarly as for *NN* scattering. As a consequence one has coupled two-dimensional equations. In the second set of equations, the well-known deuteron properties of a *S* and *D* waves content is built in and the analytical angular behavior of those amplitudes is taken into account explicitly. In this case, one arrives at one-dimensional equations. This second derivation bears some similarity to partial wave methods. The two one-dimensional amplitude components are each linear combination of the standard *S* and *D* wave function components.

The calculated deuteron binding energy determined in both ways agrees perfectly with the value determined in standard calculations based on partial wave representations of the deuteron eigenvalue equation. The newly defined helicity wave function components depend on Wigner's d function and the q dependent part are linear combinations of the standard *S* and *D* waves of the deuteron. We display their properties for different projections of the total angular momentum M_d. As for *NN* scattering we can connect the helicity amplitudes to the standard *S* and *D* waves and find perfect numerical agreement with the partial wave components determined in a standard manner.

Finally we evaluate various spin and momentum dependent probabilities in a fashion which is exact with respect to the angular dependence. This is made possible by using the ''operator form'' of the deuteron state. It is conceivable that in quasielastic electrodisintegration of the deuteron one may be able to see those momentum dependent spin distributions.

Summarizing, we extended a recently introduced helicity representation for *NN* scattering to the *NN* bound state. This formulation leads to new forms for deuteron wave function components, which can be determined by two coupled equations.

ACKNOWLEDGMENTS

This work was performed in part under the auspices of the Deutsche Akademische Austauschdienst under Contract No. A/96/32258, the U. S. Department of Energy under Contract No. DE-FG02-93ER40756 with Ohio University, the NATO Collaborative Research Grant No. 960892, and the National Science Foundation under Grant No. INT-9726624. We thank the Neumann Institute for Computing (NIC) at the Forschungzentrum Jülich and the Computer Center of the RWTH Aachen (Grant No. P039) for the use of their facilities. We especially thank H. Schumacher from NIC for his assistance with the three-dimensional images.

[1] I. Fachruddin, Ch. Elster, and W. Glöckle, Phys. Rev. C **62**, 044002 (2000).
[2] M. Jacob and G.C. Wick, Ann. Phys. (N.Y.) **7**, 404 (1959).
[3] R. Alzetta, K. Erkelenz, and K. Holinde, Nucl. Phys. **A185**, 459 (1972).
[4] R. Machleidt, Adv. Nucl. Phys. **19**, 189 (1989).
[5] J.L. Forest, V.R. Pandharipande, S.C. Pieper, R.B. Wiringa, R. Schiavilla, and A. Arriaga, Phys. Rev. C **54**, 646 (1996).
[6] R.B. Wiringa, V.G.J. Stoks, and R. Schiavilla, Phys. Rev. C **51**, 38 (1995).
[7] T. Ericson and W. Weise, *Pions and Nuclei*, The International Series of Monographs in Physics No. 74 (Clarendon, Oxford, 1998), p. 49.
[8] P.L. DeVries, *A First Course in Computational Physics* (Wiley, New York, 1994).
[9] R.A. Malfliet and J.A. Tjon, Nucl. Phys. **A127**, 161 (1969).
[10] W. Glöckle, Nucl. Phys. **A381**, 343 (1982).
[11] M. E. Rose, *Elementary Theory of Angular Momentum* (Wiley, New York, 1957).